Article

Unraveling the Role of a Flexible Tetradentate Ligand in the Aerobic Oxidative Carbon-Carbon Bond Formation with Palladium Complexes: A Computational Mechanistic Study

Qian Peng, Zengwei Wang, Snezana D. Zaric, Edward N. Brothers, and Michael B. Hall

J. Am. Chem. Soc., **Just Accepted Manuscript** • DOI: 10.1021/jacs.7b11701 • Publication Date (Web): 14 Feb 2018

Unraveling the Role of a Flexible Tetradentate Ligand in the Aerobic Oxidative Carbon-Carbon Bond Formation with Palladium Complexes: A Computational Mechanistic Study

Qian Peng[1,2]*, Zengwei Wang[1], Snežana D. Zarić[3,4], Edward N. Brothers[3], and Michael B. Hall[2]*

1. State Key Laboratory of Elemento-Organic Chemistry, College of Chemistry, Nankai University, Tianjin 300071, China. E-mail: qpeng@nankai.edu.cn
2. Department of Chemistry, Texas A&M University, College Station, TX 77843-3255 e-mail: mbhall@tamu.edu, Tel +1-979-845-1843, Fax: +1-979-845-2971
3. Department of Chemistry, Texas A&M University at Qatar, P.O. Box 23874, Doha, Qatar
4. Department of Chemistry, University of Belgrade, Studentski trg 12-16, Belgrade, Serbia

Abstract:

Mechanistic details of the aerobic oxidative coupling of methyl groups by a novel (^{Me}L)Pd^{II}(Me)$_2$ complex with the tetradentate ligand ^{Me}L = N,N-di-methyl-2,11-diaza[3.3](2,6)pyridinophane has been explored by density functional theory (DFT) calculations. The calculated mechanism sheds light on the role of this ligand's flexibility in several stages of the reaction, especially as the oxidation state of the Pd changes. Ligand flexibility leads to diverse axial coordination modes and it controls the availability of electrons by modulating the energies of high-lying molecular orbitals, particularly those with major d_{z^2} character. Solvent molecules, particularly water, appear essential in the aerobic oxidation of Pd(II) by lowering the energy of the oxygen molecule's unoccupied molecular orbital and stabilizing the Pd-O_2 complex. Ligand flexibility and solvent coordination to oxygen are essential to the required spin-crossover for the transformation of high-valent Pd^X-O_2 complexes. A methyl cation pathway has been predicted by our calculations in transmetalation between Pd^{II} and Pd^{IV} intermediates to be preferred over methyl radical or methyl anion pathways. Combining an axial and equatorial methyl group is preferred in the reductive elimination pathway where roles are played by the ligand's flexibility and the fluxionality of trimethyl groups

INTRODUCTION

Ring flipping as defined by the conformational analysis of cyclohexane, is a interconversion phenomenon arising from low barrier rotations about single bonds in this cyclic molecule[1]. Ring flipping in multidentate flexible ligands enables the formation of complexes with variable coordination numbers. Although ligand flexibility, to one degree or another, often occurs in coordination chemistry, little attention has been focused on how such conformational changes might lead to significant effects on the chemistry. An exception is the evolution of the DuBois catalyst,[2] a well-known H_2 catalyst, where each of several coordination spheres of the active Ni core and their flexibility play a crucial role in the efficiency (TOF increase from < 0.2 s^{-1} to 1.1×10^5 s^{-1}).

Scheme 1. A) Proposed catalytic cycle for Pd-catalyzed methyl dimerization; B) examples of complexes performing aerobic oxidation of $Pd^{II}Me$

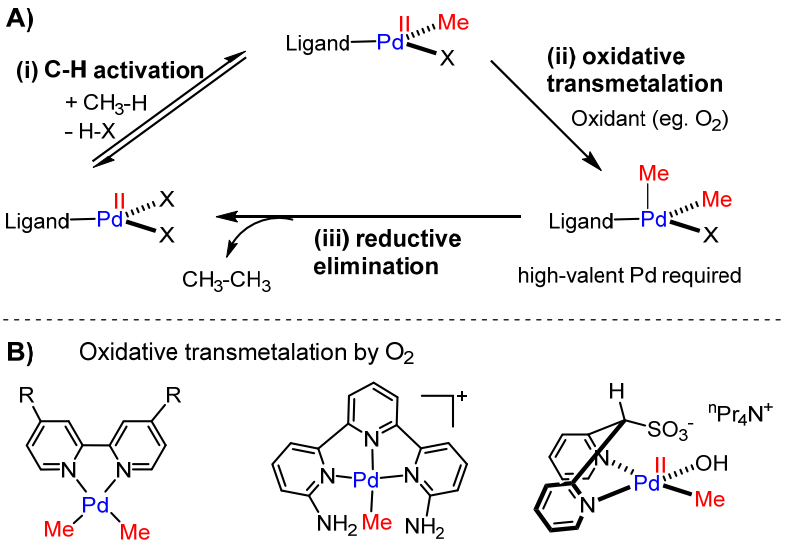

Although the catalytic oxidative coupling of methane is an attractive route to ethane and higher hydrocarbons[3], such oxidation reactions with molecular oxygen are rare; rarer still are studies on how ligand flexibility might improve such industrially important reactions. Palladium complexes have been widely applied as efficient catalysts

for the C-C coupling reactions in synthetic chemistry.[4] The vast majority of these reactions involve Pd^{0}/Pd^{II} catalytic cycles with assistance of either a functionalized substrate[5] or a sacrificial oxidant[6,7a]. Molecular oxygen, as an environmentally friendly and inexpensive oxidant, is a desirable reagent for a variety of oxidative organic transformations[7-8]. Although various high-valent oxidants (Pd^{IV} and/or Pd^{III}) have been employed in catalyzing C-C coupling reactions[9], very few C-C bond formation reactions have been induced by aerobic oxidation of Pd^{II} precursors (leading to formation of experimentally detectable Pd^{III} or Pd^{IV}).[10] The proposed catalytic cycle with ethane release includes the challenging steps in Scheme 1A, where transmetalation (step ii) requires a strong oxidant to enable formation of high-valent Pd species. The reductive elimination from dimethyl Pd^{II} is slow[11], hence oxidation to high-valent Pd species are necessary to promote this step to yield ethane. Very few examples of ligands have been reported to facilitate the reactions between O_2 and $Pd^{II}Me$,[12] which also limit the development of aerobic oxidation for the transmetalation step.

Scheme 2. Proposed mechanism for aerobic oxidatively induced reductive elimination of ethane from the Pd^{II} dimethyl complex showing possible coordination modes of the ligand L. In the text we used shorthand notations **N2** (for κ^2-L), **N3** (for κ^3-L), and **N4** (for κ^4-L).

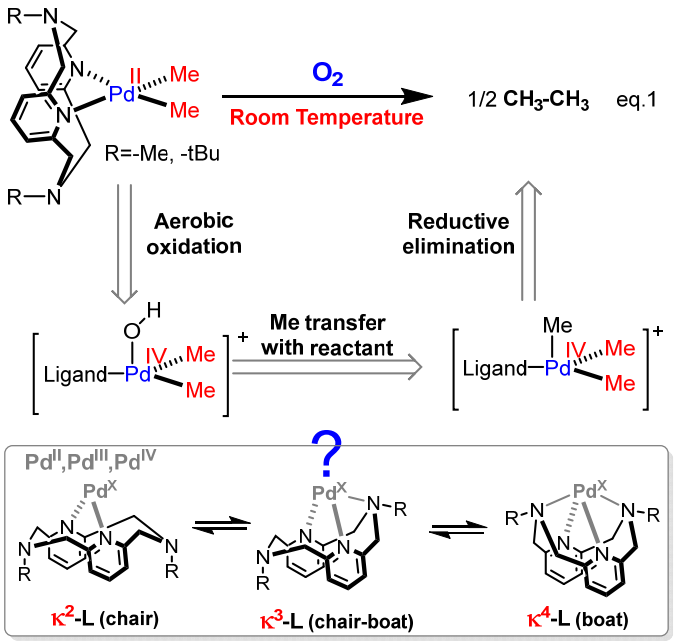

Recently, Mirica and his coworkers reported successful steps in the aerobic oxidative catalysis of methane to ethane with a palladium catalyst featuring a new tetradentate ligand (Scheme 2, eq 1)[13]. In the catalytic cycle, after the C-H bond activation that forms L-$Pd^{II}(Me)_2$, oxidation of this complex with molecular oxygen leads to the formation of ethane at room temperature. The authors presented a tentative mechanism for which they have identified many of the intermediates or provided spectroscopic evidence of them. In their mechanism[13], the initial L-$Pd^{II}(Me)_2$ complex is oxidized by O_2 to form a [Pd^{III}-O-O] complex, whose existence was supported by EPR of DMPO adduct. The peroxide bond cleavage process leads to the [Pd^{IV}-OH]$^+$ complex, which is the key intermediate for Me group transfer. Possible [Pd^{III}] complexes had also been proposed to generate tri-methyl [Pd^{IV}]$^+$, which was proven to be the precursor for reductive elimination to liberate ethane. Such a facile reaction is unprecedented, and these tetradentate ligands or their analogues have been applied to other interesting reactions by high-valent metals.[14] Therefore, understanding the mechanism in detail would be useful in order to control and improve such aerobic reaction under mild condition. Unveiling the role of ligand flexibility may suggest other ways to promote oxidation reactions employing mild oxidants.

Although tremendous effort was expended and much was achieved in the mechanistic study by Mirica's group[13], several critical issues remain unclear. (1) The crossover experiments imply that the Pd^{III} complex exhibits low reactivity compare to initial Pd^{II} complex, a conclusion which seems discordant with the status of Pd^{III} complexes in the tentative mechanism; (2) The reaction is unlikely to be controlled by a non-metal-based radical mechanism, but how does a Me group transfer via a possible metal radical of the Pd^{III} complex? What is the state of the Me group during such process, cation, radical, or anion? (3) The experimental studies during the solvent optimization[13b] indicate that the reaction rates are accelerated by increasing the concentration of H_2O in the mixed solvent, H_2O/CH_3CN, but the role of H_2O in this reaction is obscure. (4) Recently, Mirica's group proved that the conformational flexibility of the tetradentate ligand is essential for the stabilization of the Pd^{III} complex with low oxidation potential[15]. Hence, it is intriguing to investigate how this conformational flexibility affects the entire reaction.

In this paper, we use density functional theory (DFT) calculations to examine the mechanistic issues mentioned above and to gain insight into aerobic oxidative coupling by high-valent Pd. This study provides a route to understand the reliability of these calculations through comparisons with experimental observations.[16]

RESULTS AND DISCUSSION

a. The ligand's flexibility and its role in key intermediate complexes

Initial calculations were performed to investigate the ligand flexibility alone and in key intermediates that had been detected experimentally, dimethyl Pd^{II}, dimethyl Pd^{III}, and trimethyl Pd^{IV}. The calculated structures and energies for three stable coordination modes corresponding to three conformations, namely κ^2-L (chair), κ^3-L (chair-boat) and κ^4-L (boat), are shown in Figure 1 (see SI for more $Pd^{(IV)}$ complexes on ligand flexibility and flipping). The short notation: **N2** for κ^2-L, **N3** for κ^3-L, and **N4** for κ^4-L (Scheme 2) reflects the number of ligand N atoms coordinated to the metal, except for Pd^{IV}_N4,

where the fourth N cannot coordinate to Pd because the axial coordination site is occupied by Me and OH in $Pd^{IV}Me_3$-L and $Pd^{IV}Me_2(OH)$-L, respectively.

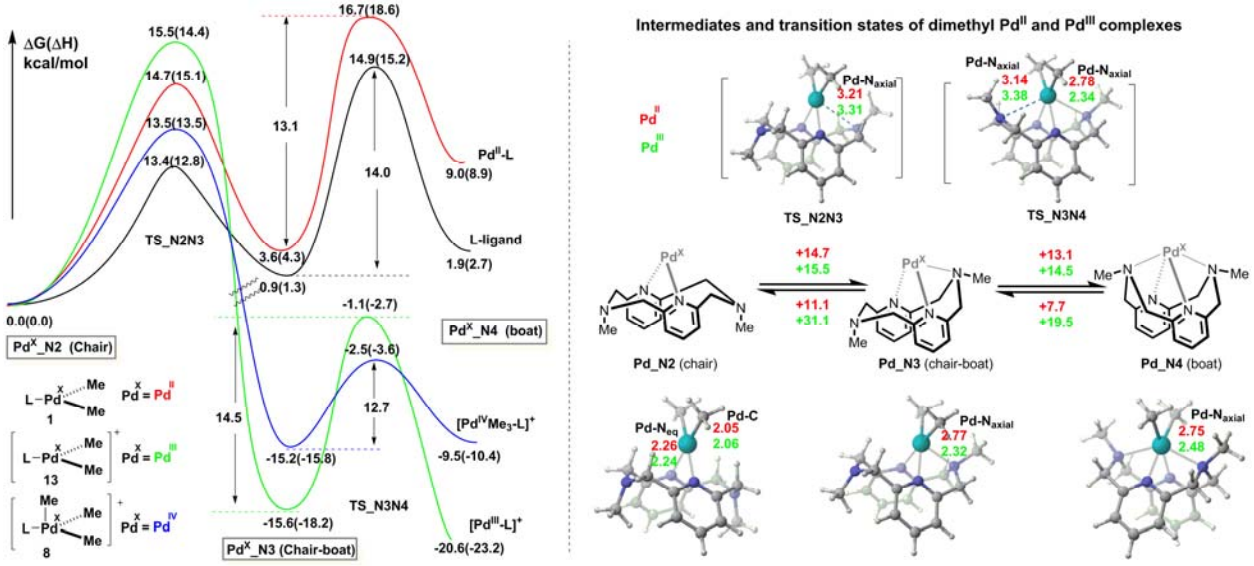

Figure 1. Energy profiles of ligand conformations and coordination modes in various complexes (left panel); and related structures and energies of dimethyl Pd^{II} and Pd^{III} complexes (right panel). Free ligand ^{Me}**L** (L-ligand, black line); ^{Me}**L**$Pd^{II}Me_2$ complex (Pd^{II}-L, red line); $[^{Me}$**L**$Pd^{III}Me_2]^+$(Pd^{III}-L, green line); $[^{Me}$**L**$Pd^{IV}Me_3]^+$($Pd^{IV}Me_3$-L, blue line); bond lengths shown in Å and energy shown in kcal/mol.

Calculations on ligand itself show very small decrease in stability from **N2**(chair), to **N3** (chair-boat) and to **N4** (boat) conformations with conversion barriers < 15 kcal/mol (Figure 1, black line), such barriers provide facile transformations at room temperature. The trend was similar for the dimethyl Pd^{II} complexes with the **Pd^{II}_N2** conformation as the most stable, but with a much larger decrease in stability for the **Pd^{II}_N4** conformation and a modest increase in the conversion barriers (Figure 1, red line). Due to fully occupied d_{z2} orbital of Pd^{II}, the Pd to N_{axial} distances in **Pd^{II}_N3** and **Pd^{II}_N4** complexes are quite long about 2.7 Å. This weak, slightly repulsive interaction is responsible for the decreasing stability trend. Since Pd^{III} and Pd^{IV} have half empty and empty d_{z2} orbital, respectively, additional axial coordination is favored here. In **Pd^{III}_N3** the Pd-N_{axial} bond shortens to 2.3 Å and this complex is 19.2 kcal/mol more stable (relatively) than the **Pd^{II}_N3** complex. While the **Pd^{III}_N4** is significantly more stable

than the **Pd^{III}_N3** , the **Pd^{IV}_N4** is somewhat less stable than the **Pd^{IV}_N3** from the steric crowding of the third Me group. The stabilization of the N3 conformations for both Pd^{III} and Pd^{IV} complexes inhibits transformation from N3 to N2 (backward barrier >28 kcal/mol), while the barriers for transformation between N3 and N4 are much lower, especially for trimethyl Pd^{IV} complex with the sterics involved.

b. Mechanism for Aerobic Oxidation of (^{Me}L)Pd^{II} complex to high-valent Pd

Despite the importance of O_2 activation, there are very few computational studies on aerobic oxidation of Pd catalysts, most of which operate through Pd^0/Pd^{II} cycles[17], while Pd^{II}/Pd^{IV} cycles are usually more unfavorable.[17b] Recently, Stahl and co-workers reported that the diazafluorene ligand promoted a variety of diverse coordination modes for ligated Pd^{II} complexes during aerobic oxidation reactions, implying the important contribution of flexible coordination geometries.[18] Mirica and co-workers[13] also found that the flexibility of their tetradentate ligand played key roles in their Pd^{II} aerobic oxidations. In addition, they examined the nature of the reaction of O_2 with their ^{Me}LPd^{II}Me$_2$ complex and reported the formation of a [Pd^{III}-O-O] complex, whose DMPO adduct was observed by EPR.

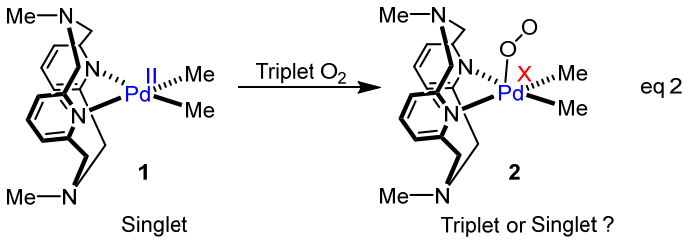

eq 2

This computational study, to unravel the mechanism of the Pd catalyst's aerobic oxidation and the role of ligand flexibility in the mechanism, begins with an examination of the complex's reaction with O_2. The interaction of singlet Pd^{II}-N2 complex with triplet-O_2 could result in either singlet or triplet state complex, **2** (eq. 2). Note that singlet could be Pd^{II}-N2-O_2 or Pd^{IV}-N2-O_2^{2-}, while the triplet would be Pd^{III}-N2-O_2^{-}. In our DFT calculations, the singlet complex **2** was obtained without any constrains, by forming a terminally coordinated complex, with a Pd...O bond of 2.29 Å. The energies of closed-

shell singlet, as well as the single point energies of triplet and open-shell singlet states, at the optimized singlet structure along the Pd-O reaction coordinate distance, are shown in Figure 2. The single point energies of triplet and open-shell singlet states are 17.3 kcal/mol and 11.4 kcal/mol more stable than closed-shell singlet state, respectively. Interestingly, the triplet complex **2** favors dissociation of O_2; because of this rather weak interaction between Pd^{II} and O_2, a fully optimized triplet state has a Pd...O distance of 4.01 Å. Various DFT functionals and coordination modes (e.g. O_2 side coordination) of Pd^{II}-N2 have been tested to better evaluate the relative energies of spin states and structures (See SI). All the calculations indicate that the unstable Pd^{II}-N2-O_2 triplet state is the lowest in energy. Thus, the question arises, how can triplet O_2 approach and interact with Pd^{II} to form a complex that is stable enough to be trapped by DMPO.

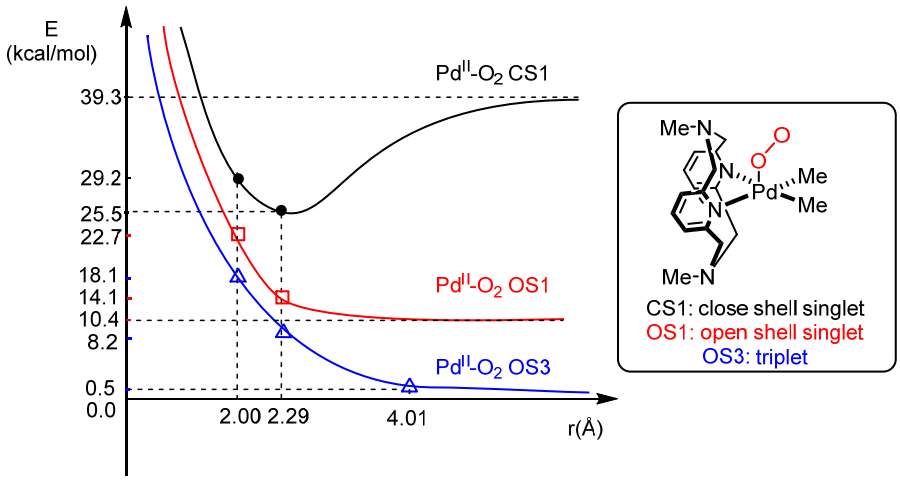

Figure 2. Electronic energy as function of Pd-O distances of different spin states of **Pd^{II}-N2**-O_2 with basis set superposition error (BSSE) corrections.

The lack of driving force to form a Pd-O_2 triplet complex in our calculations led us to calculate ^{Me}**L**Pd-O_2-DMPO that had been observed as ^{Me}**L**Pd^{III}-O_2^- adduct by EPR spectra in Mirica group[13]. We obtained stable triplet states with reasonable Pd-O bond distances of 2.28 Å and 2.26 Å in **3-N2** and **3-N3**, respectively (Scheme 3). The triplet states are more stable than the singlet states, in agreement with experimental observation of the ^{Me}L-Pd^{III}-O_2-DMPO• adduct. Thus, introducing dimethyl pyridine N-oxide (DMPO), a commonly used spin trap for O-centered radicals, is important to stabilize the triplet

state of the Pd-O_2 complex. However, it is still obscure whether the actual ^{Me}L-Pd-O_2 triplet complex is formed in this aerobic reaction without DMPO. A rational explanation should be that some effects in the reaction itself stabilized the triplet Pd-O_2 adduct inhibiting the O_2 dissociation long enough for further reactions to occur.

Scheme 3. Relative energies of ^{Me}LPd^{II}-O_2-DMPO adduct. DMPO combined with O_2 dissociate from Pd center. $\Delta E_{(S)}$: relative energies of singlet states, $\Delta E_{(T)}$: relative energies of triplet states. The distances of Pd-O, O-O and Pd-N_{ax} are depicted in the structures. All units of energies and distances throughout our paper are shown in kcal/mol and Å, respectively.

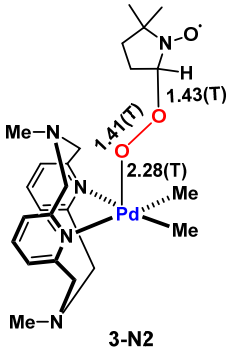

3-N2

3-N2	Complex	3-N3
$\Delta E_{(S)}$[a]= 0.0	relative energy (kcal/mol)	$\Delta E_{(S)}$= 12.5
$\Delta E_{(T)}$= -7.1		$\Delta E_{(T)}$= -6.6

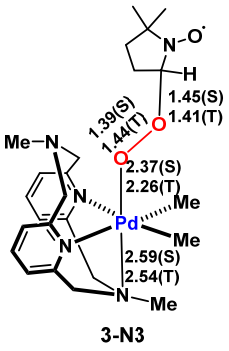

3-N3

According to Mirica's experimental observations, the reaction was realized when a solution of reactant, dimethyl ^{Me}L-Pd^{II} complex, **1,** is exposed to O_2 or air in the presence of protic solvents (like H_2O, MeOH). Presence of protic solvents provides a potential clue to understand the mystery of a triplet Pd-O_2 complex. To examine the effects of such solvents, the calculated structures were fully optimized in the SMD solvent model with additional explicit protons and solvent molecule(s), such as H^+, H_2O, H_3O^+, $(H_2O)_2$ and $(H_2O)_3$. The data show that Pd-N3-O_2 triplet complex is stabilized by H_2O molecules (Figure 3 and Figures in SI). The Pd-O bond distances is 3.10 Å in **2_N3**, while it is significantly shorter, 2.55 Å, in **2_N3_$(H_2O)_3$**. Simultaneously, the spin density increases from 0.137 to 0.462, while energy difference between the singlet and triplet states decreases, from 9.4 kcal/mol in **2_N3** to 0.6 kcal/mol in **2_N3_$(H_2O)_3$** (Figure 3A). However, explicit H_2O did not stabilize the Pd-N2-O_2 triplet complex, as the data on the Pd-O bond distances of **2_N2** and **2_N2_$(H_2O)_3$** show (Figure 3B and 3C).

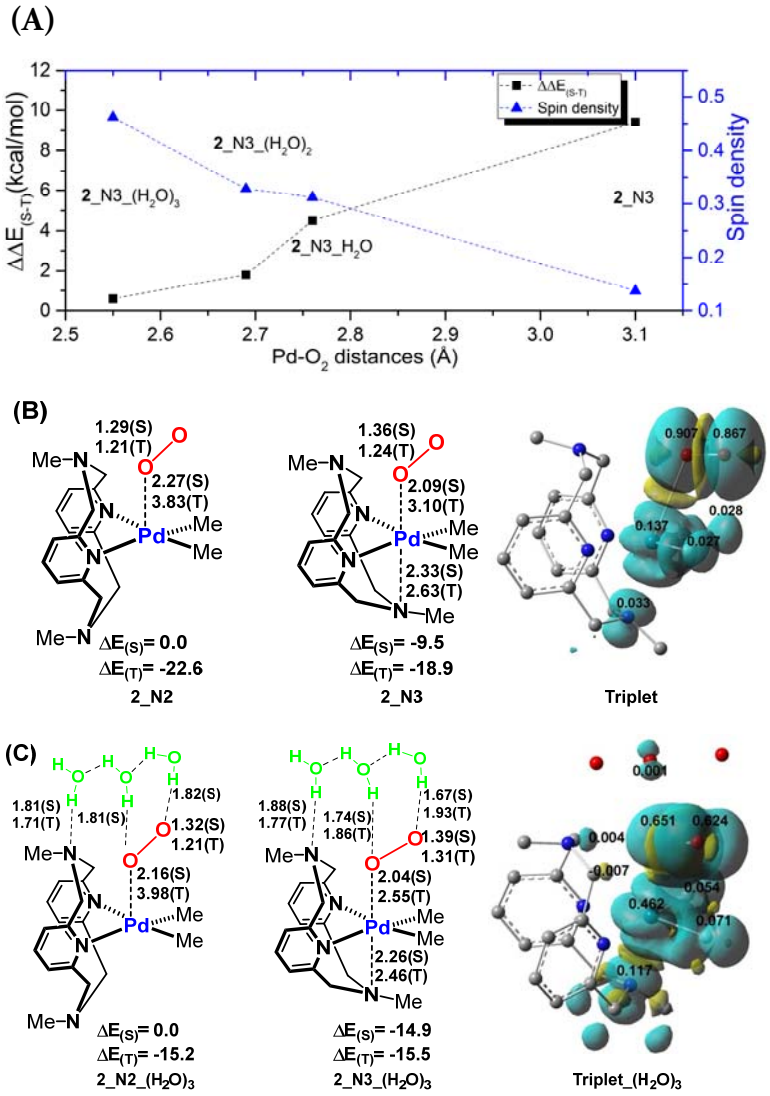

Figure 3. Explicit solvent models of ^{Me}LPd^{II}-O_2 complexes **2** with two N (**N2**) and three N (**N3**) coordinated to Pd. (A) the trend of $\Delta E_{(S-T)}$ and spin density on Pd with Pd-O_2 distances in testing complex **2**, $\Delta\Delta E_{(S-T)} = \Delta E_{(S)} - \Delta E_{(T)}$.; (B) **N2** and **N3** structures and spin density of complex **2** without H_2O; (C) **N2** and **N3** structures and spin density of complex **2** with three H_2O molecules.

In order to form a triplet complex with reasonably strong Pd-O bonds, two key factors are needed: (1) axial N coordination (N_3 structure) and (2) explicit solvent involvement. First, **2_N2_$(H_2O)_3$** without axial N coordination will dissociate O_2 from the low energy triplet complex with a long Pd-O distance of 3.98 Å (Figure 3C). Second, **2_N3** without

H_2O forms only a weak interaction between Pd and O_2 with a Pd-O distance of 3.10 Å (Figure 3B). However, when both key factors are involved as in **2_N3_$(H_2O)_3$**, the Pd-O bond distance is significantly shorter, 2.55 Å and the complex is stabilized. Similar results are produced by using explicit MeOH as a protonic source, and the triplet 2_N3_$(MeOH)_3$ complex shows a reasonable Pd-O distance of 2.47 Å and spin density on Pd of 0.493, see Figure S7.

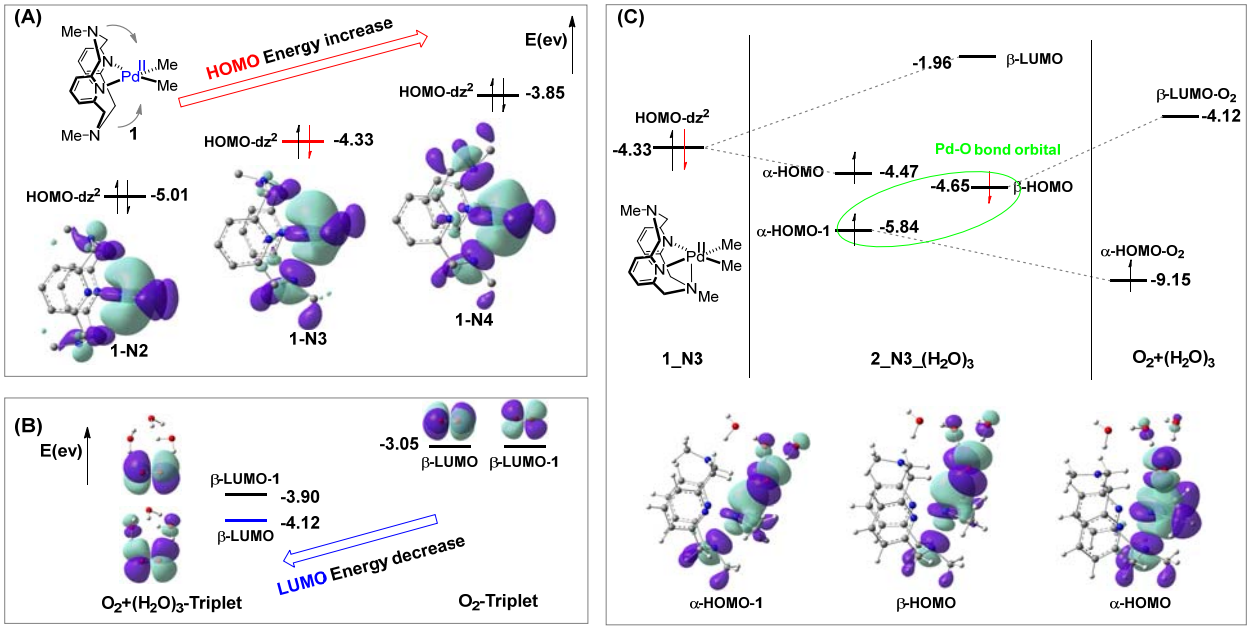

Figure 4. Frontier orbitals of $(^{Me}\mathbf{L})Pd^{II}Me_2$ complex **1** reacting with triplet O_2. (A) Frontier orbitals (HOMOs) of complex **1** with various coordinations; (B) frontier orbitals of triplet O_2 with/without H_2O involved; (C) Molecular diagram for forming the $(^{Me}\mathbf{L})Pd^{II}Me_2$-$O_2(H_2O)_3$ triplet complex (**2_N3**).

To rationalize and understand how these two significant factors, axial N coordination and an explicit solvent H_2O, work together, the frontier orbitals of $^{Me}\mathbf{L}Pd^{II}$ and O_2 were examined (Figure 4). The energies of HOMOs in $^{Me}\mathbf{L}Pd^{II}$ are highly depend on the axial coordination of N ligand because the d_{z^2} character of the complex's HOMO make it sensitive to changes along the axial directions. Coordination of the first axial N increases the HOMO's energy by 0.68 eV, while coordination of the second increases its energy by

an additional 0.48 eV. These energy increases can be ascribed to the electronic repulsion between the lone pair of the axial N(s) and the d_{z^2} HOMO on Pd. The coordination of second axial N in **2_N4** will full occupy the available position and will block O_2 access; therefore **2_N4** will inhibit the aerobic reaction. The β-LUMOs of O_2 are the anti-bonding orbitals (π*) which may accept electrons from the Pd complex's HOMOs (Figure 4). Due to the relatively high-energy gap in these frontier orbitals, **2_N3** has only a weak interaction between Pd and O_2 reflected by spin density locating on Pd of 0.137 (Figure 3B). Introducing explicit water molecules $(H_2O)_3$ in the model decreases the O_2 β-LUMO's energy from -3.05 eV to -4.12 eV and leads to a more favorable energy gap (Figure 4B). Also, the spin density on Pd and axial N increases to a total of 0.579, more reflective of Pd^{III}–O_2^- in **2_N3_$(H_2O)_3$** (Figure 3C). A diagram of the frontier orbitals in Figure 4C illustrates the nature of bond formation in triplet **2_N3_$(H_2O)_3$**, where α-HOMO-1 and β-LUMO were paired to form Pd-O bonding orbital of complex **2_N3_$(H_2O)_3$**, which is seen in the orbital contours The remaining two single electrons are in Pd-O anti-bonding (α-HOMO, hence Pd^{III}) and an O-O anti-bonding orbital (α-HOMO-2, hence O_2^-) that confirms **2_N3_$(H_2O)_3$** as a triplet state ^{Me}**L**$Pd^{III}Me_2$-O_2^-. Thus, both axial coordination of the third N and explicit solvent are necessary to form ^{Me}**L**$Pd^{III}Me_2$-O_2^-, protonic solvents are particularly good at this stabilization, hence the importance of H_2O or MeOH in this reaction.

c. Peroxide oxidation of complex with spin crossover and O-O bond breaking

The ESI-MS spectra imply complexes **3** and **7** **(eq. 3)** as intermediates in the reaction mechanism[13], however, the transformation of triplet complex **2** to singlet **3** and finally to singlet **7** it remains unclear**.** There are possible spin crossovers from **2** to **3** (Figure 5) and O-O bond breaking from **3** reacting with **1** to form **7** as shown in Figure 6.

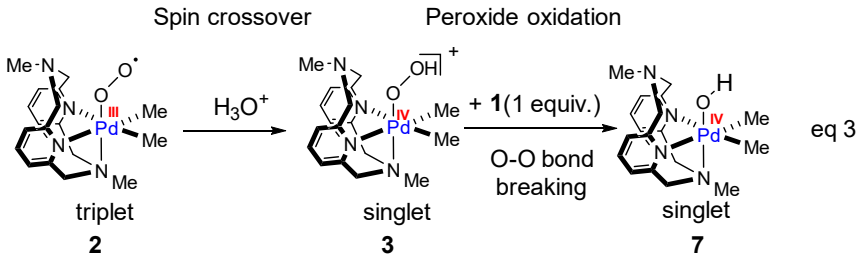

eq 3

As illustrated above, explicit solvent interactions are essential to stabilizing the triplet complex **2_N3** and strengthening the Pd-O bond and preventing the complex's dissociation. As shown in Figure 5 (and Figure SI), these solvent interactions also stabilize the singlet state even more effectively, finally bringing the singlet and triplet state of the **2_N3** O2 complex to nearly the same energy. As explicit H_2O molecules are added, the barrier to spin crossover drops in electronic energy from 10.0 kcal/mol in **2_N3** to 2.2 kcal/mol in **2_N3_(H₂O)₃** and Pd-O bond lengths at spin crossover point elongates. Further inspection of the **2_N3_(H₂O)₃** structures (Figure 3C) shows that the hydrogen bonds between O_2 and H_2O in the complex are stronger for the singlet than for the triplet, indicating quite efficient hydrogen bond formation in the singlet but not in the triplet. Moreover, the hydrogen bond to the terminal O (1.67 Å) is stronger than that to the central O (1.74 Å) in the singlet, in contrast to the triplet state with 1.93 Å to the terminal and 1.86 Å to the central O. Therefore, introduction of H_3O^+ shows significantly stronger stabilization for the singlet state (see SI).

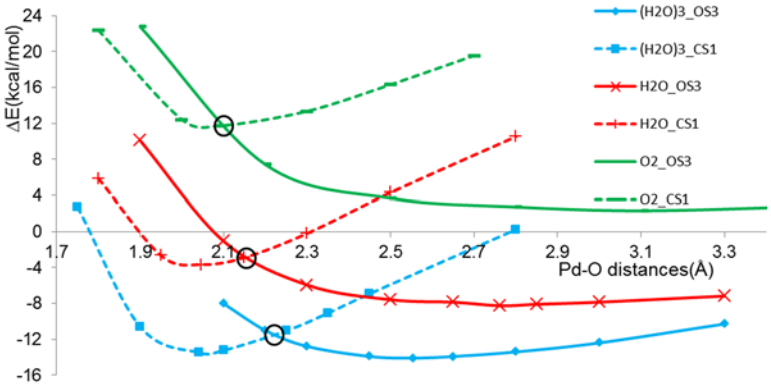

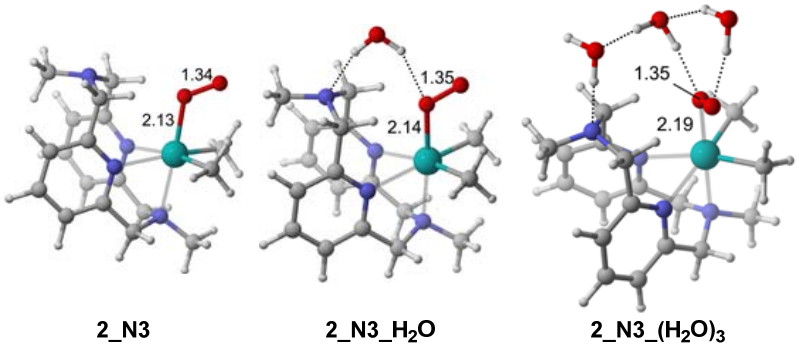

Figure 5. Energy profile for the oxygenation of ^{Me}**L** $Pd^{II}Me_2$_N3 to form the complexes **2_N3_(H₂O)$_x$** involving explicit H_2O. Dash lines show the singlet energy surfaces (CS1), solid lines show the triplet energy surfaces (OS3). Calculated structures of the spin-crossover point between S=1 and S=0 are shown in lower panel.

The calculated free-energy profile of peroxide oxidation process involves two complex species as shown in Figure 6. The profile shows that the process of O-O bond breaking is more than 60 kcal/mol exergonic with an activation barrier of 18.0 kcal/mol. The optimized transition state (**TS5**) appears to be an early transition state, reflected by Pd-O distance of 2.81 Å and O-O bond of 1.57 Å. In this process the Pd^{IV} complex **3** smoothly oxidizes the reactant Pd^{II} complex **1** to two Pd^{IV} complexes **7** that are the key intermediate for intermolecular Me transfer leading to the tri-methyl Pd^{IV}.

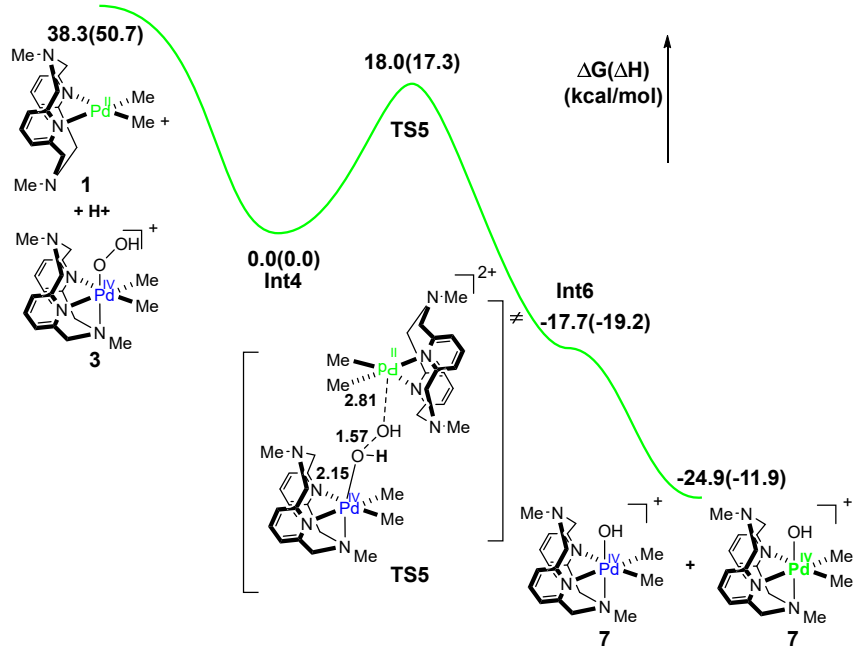

Figure 6. Energy profile of peroxide O-O breaking process, bond distance shown in Å.

d. Mechanisms of intermolecular Me transfer to form $^{Me}LPd^{IV}Me_3$

Scheme 4. Three proposed mechanism for Me transfer

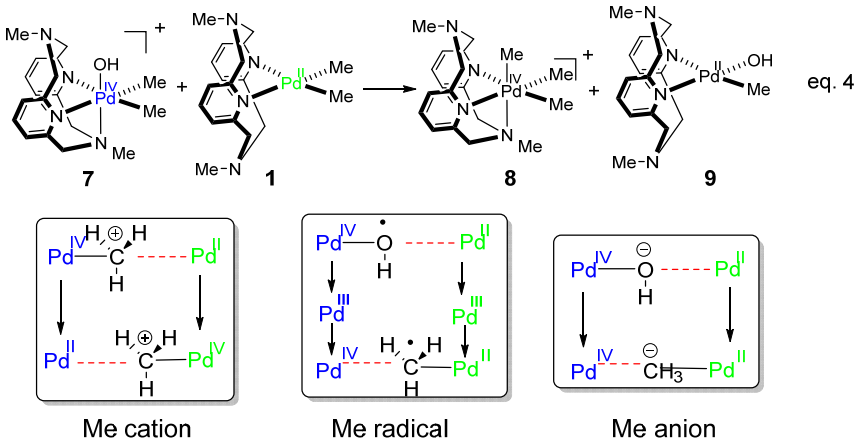

Direct reductive elimination of ethane from dimethyl Pd^{II} is slow[11], however, high-valent Pd^{IV} species promote this step to yield ethane with the assistance of bidentate[19] and tridentate ligands[12c]. In Mirica's reaction, the $[^{Me}LPd^{IV}Me_3]^+$ complex **8** (eq. 4) was experimentally detected and shown to be the key intermediate for the reductive elimination[13]. However, the mechanism of obtaining the trimethyl species **8** from species **7** remained unknown. Based on the proposed mechanisms in experimental work, three plausible pathways, with changes of valence states on Pd, are shown in Scheme 4; Me cation, Me radical, and Me anion. Because no vacant coordination sites are available in complex **7**, possible mechanisms were proposed to transfer relevant species between complex **7** and complex **1**.

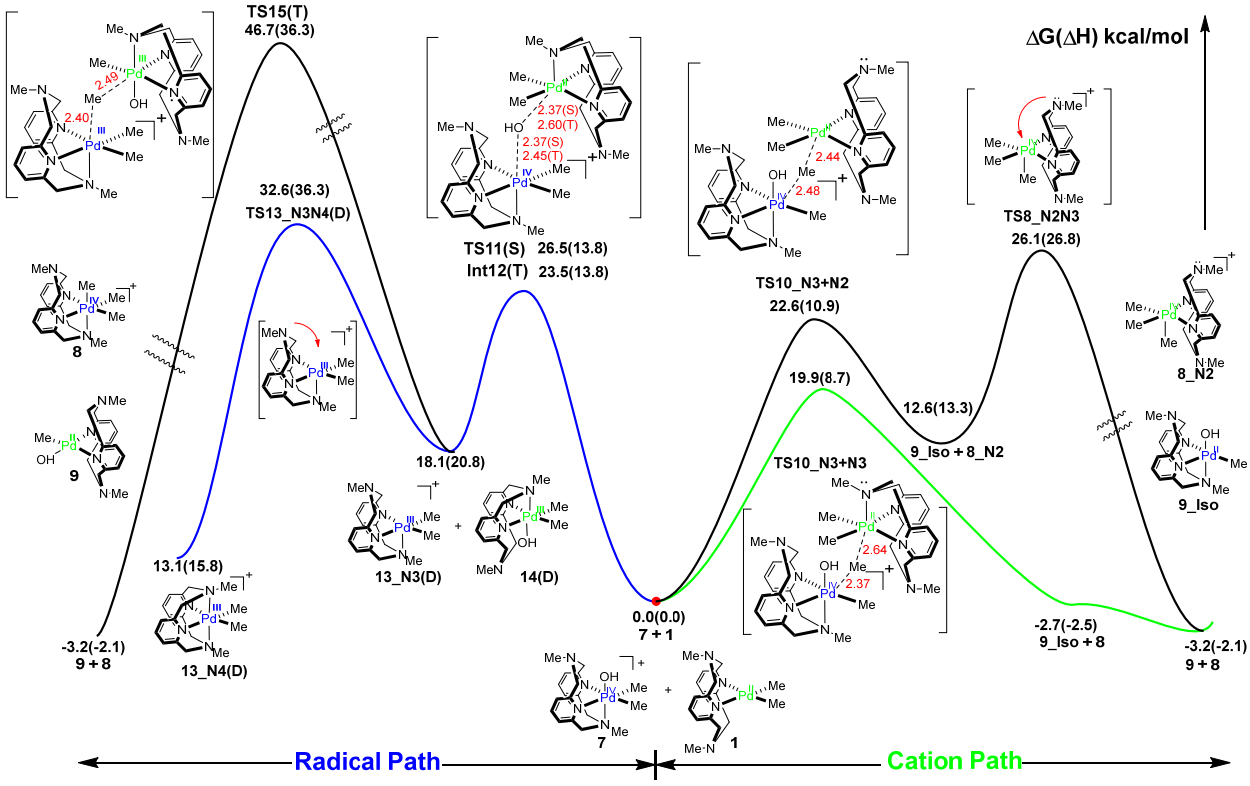

Figure 7. Energy profile of intermolecular Me transfer to form ^{Me}LPd$^{(IV)}$Me$_3$, involving possible ligand flexibility of the tetradentate ligand. Most of the structures were optimized in singlet state (S) except for those shown as D (doublet) and T (triplet). Bond distance for transition states shown in Å, energies are in kcal/mol.

First, the 'Me anion' pathway is ruled out by our initial calculations showing that dissociating OH^- from **7** would require rather high activation energy (45.9 kcal/mol in free energy with solvent correction), which is impossible at room temperature. The 'Me radical' and 'Me cation', as two competitive pathways, were investigated in detail and their energy profiles are shown in Figure 7. The comparison of two pathways shows that 'Me cation' pathway (green line in Figure 7) is most favorable when complex **1** gains axial coordination of the ligand **L (1_N3)** beginning with the transition state**.** This Me cation transfer crosses a 19.9 kcal/mol free-energy barrier via a rather early transition state (**TS10_N3+N3**, with the Pd^{IV}-Me transferring at a distance of 2.37 Å) and forms a thermodynamically stable intermediate [Pd^{IV}Me$_3$]$^+$ **8 (8_N2)**. As we discussed before (Scheme 2 and Figure 1), the Pd^{II} complex **1** is able to easily transform between κ^2-, κ^3-

and κ^4- coordinations, which makes the transition state **TS10_N3+N3** easily available. An alternative 'Me cation' transition state (**TS10_N3+N2**), in which **1** remains an N2 complex, has a free-energy barrier of 22.6 kcal/mol with a relatively late TS (with the Pd^{IV}-Me distance of 2.48 Å). This transition state is followed by transformation of N2 to N3 coordination in trimethyl Pd^{IV} species **8**. Because of this latter transformation, the overall barrier is 26.1 kcal/mol, higher than for the case of the earlier ligand conformational change in the Pd^{II} complex **1** (19.9 kcal/mol). Hence, the pathway with **TS10_N3+N2** is less competitive (Figure 7). A cation pathway for Me transfer has also been suggested for bidentate ligand processes[19].

In calculations on the 'Me radical' pathway, the ·OH and ·Me radicals are transferred between two Pd (see proposed mechanism in Scheme 4). The Pd^{III} doublet **13** (Figure 7), as a short-lifetime intermediate, could be observed experimentally by EPR and ESI-MS[13]. The calculations indicated the two-step intermolecular transfer of ·OH and ·Me radicals between two Pd complexes; where each step has free-energy barrier over 23.5 kcal/mol (radical path in Figure 7). The overall barrier of 46.7 kcal/mol makes this pathway less possible. However, regarding the step of forming Pd^{III} doublet complex, the energy barrier for OH transfer step varies with different functionals and solvent models (i.e. M06L/CPCM: 20.1 kcal/mol, see SI for details). Thus, some of the functionals and solvent models suggest that first step of ·OH transfer to form Pd^{III} doublet **13** and **14** is possible at RT**.** Moreover, this step is reversible (the barrier in reverse direction is lower) and, in comparison to the 'Me cation' pathway, more favorable to form thermodynamically stable Pd^{IV} complex **7** and Pd^{II} complex **1.** This could rationalize the experimental observation of directly C-C formation from Pd^{III} complex without O_2. One can consider an alternative way to form the Pd^{III} doublet **13**, by single electron transfer (SET) between Pd^{IV} complex **7** and Pd^{II} complex **1** (Scheme 5); however, this step is thermodynamically unfavorable as shown in eq. 5 of Scheme 5. However, the Pd^{III} doublet **13** can be obtained from the fast SET reaction of dimethyl Pd^{IV} complex **16** and Pd^{II} complex **1** in an exergonic way, supporting by analogue complex in the experiment.[20] Computationally, we cannot find evidence for methyl transfer by a radical pathway; however, Pd^{III} species can be formed by

SET, which is in agreement with experimental data on non-metal-based radical mechanism.[13b]

Scheme 5. Single electron transfer between Pd^{IV} and Pd^{II} to form Pd^{III}

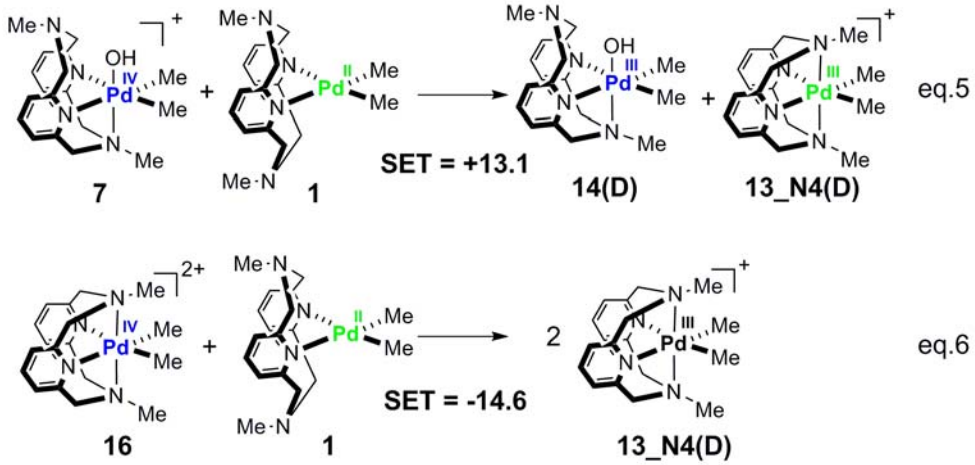

e. Ways for Reductive elimination—the fate of ^{Me}LPd^{IV}Me$_3$ complex 8

Three possible ^{Me}LPd^{IV}Me$_3$ complexes of **8,** with ligand coordination modes **8_N2, 8_N3 and 8_N4** are intermediates connected via two transition states (**TS8_N2N3** and **TS8_N3N4**) with reasonable energy barriers as shown in Scheme 6. Ligand flipping from **8_N2** to **8_N3** is irreversible (+13.5/+28.7 kcal/mol) while transformations between **8_N3** and **8_N4** are reversible with low energy barriers of +12.7/+7.0. The calculated **8_N3** is the most stable isomer, in agreement with the crystal structure of the ^{Me}LPd^{IV}Me$_3$ complex[13b]. Each of these three isomers of complex **8** can undergo reductive eliminations (RE) via transition states **TS8_RE_(N2, N3, N4)** to form thermodynamically favorable products **Pro8_(N2, N3, N4)** (Figure 9). A rather low energy barrier for RE has been located from **8_N2** suggesting that low coordination number of ligand ^{Me}**L** could benefit the RE mechanism, probably because Pd^{IV} in **8_N2** is electron deficient. This result is in agreement with the favourable RE in five coordination species found by Goldberg for Ir^{III} complexes.[21] On the other hand, RE from **8_N2** could be blocked by the high energy barrier of irreversible ligand flipping from **8_N3** to **8_N2** (28.7 kcal/mol due to Pd-N bond breaking), which is likely inoperative at RT, indicating the role of the axial coordination

in RE step in this system. Through our whole mechanism, RE would be the rate-determining step, while **8_N3** or **8_N4** would be the active species undergoing RE with reasonable and nearly equal energy barriers. Although at RT the calculated barrier is slightly high at 24.4 kcal/mol different functional produce lower barriers, such as 21.1 kcal/mol with ω-B97XD. Thus, these barriers are in reasonably good agreement with experimental observations of the long-lived intermediate **8** with $t_{1/2}$ for elimination of ethane at 68 min at RT and 6.7 days at -20°C.[13b]

Scheme 6. Energy barriers of reductive elimination from ^{Me}LPd^{IV}Me$_3$ complex **8,** considering ligand flexibility. Although in **8_N4** there are four available Ns from the ligand, the fourth N cannot coordinate to Pd because its axial coordination has been blocked by Me.

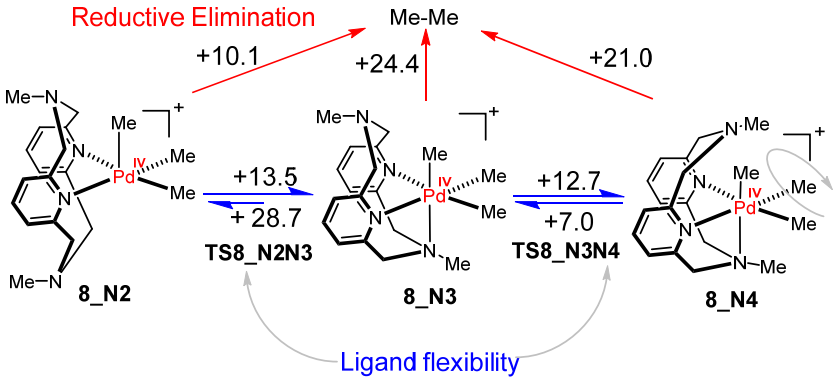

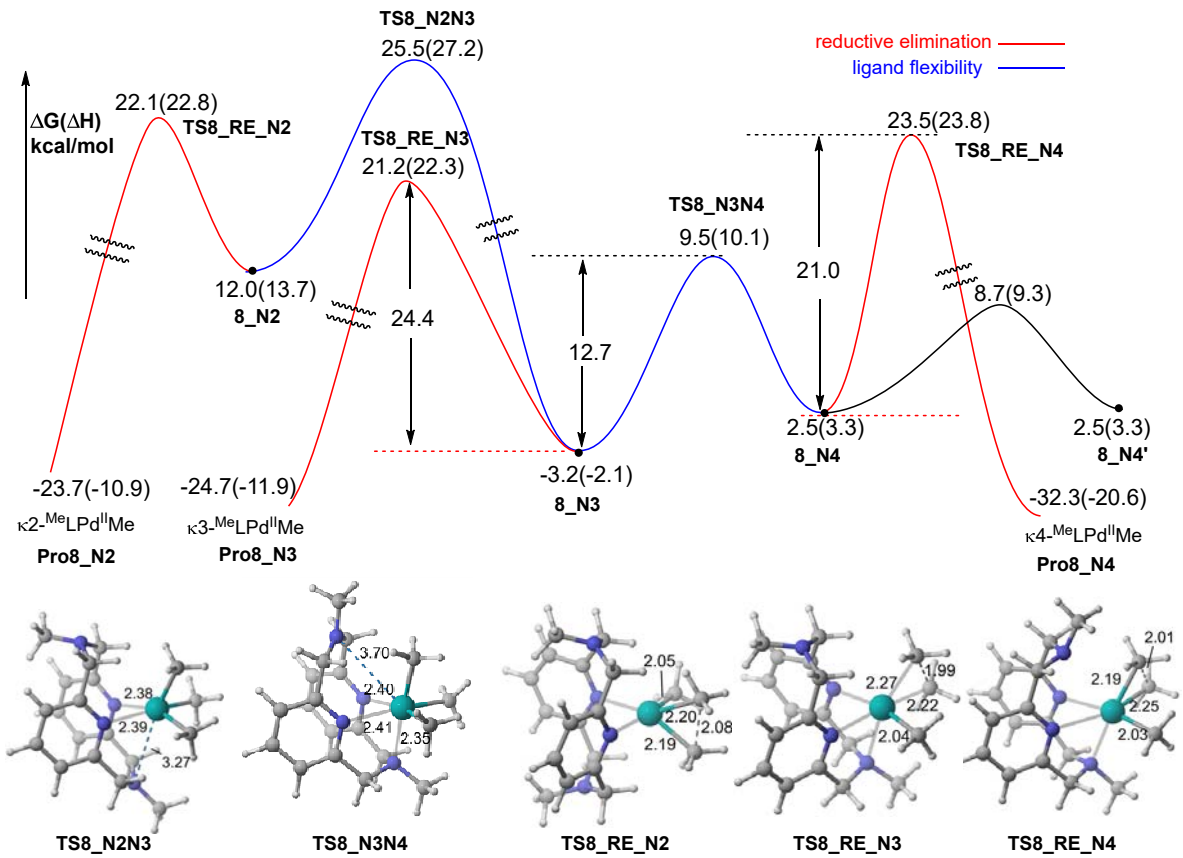

Figure 8. Energy profiles of reductive elimination (red line) combined with ligand flipping (blue line). Rotation of the three Me group is shown in black line. Structures of TSs are shown in lower panel. The "Pro" label is used for precursors of products.

The low rotation barrier (6.2 kcal/mol) among the three Me group of **8_N4** lead to the same isomer **8_N4'**, in which the axial and equatorial Me groups have exchanged. This fluxionality was observed experimentally and plays a role in the distribution of products from isotopically labeled reactants[13], since in the reductive elimination mechanism axial-equatorial pairs are always eliminated.[22] Theses mechanistic path can be rationalized by looking at the orbitals. During the elimination of two methyl groups, two electrons need to refill an orbital on Pd bringing it back to Pd^{II}; refilling in dz^2 through an axial-equatorial RE is much more favorable than refilling the dx^2-y^2 through an equatorial-equatorial RE because the dz^2 orbital is more stable than the dx^2-y^2 (Scheme 7) .

Scheme 7. Comparison of axial elimination and equatorial elimination

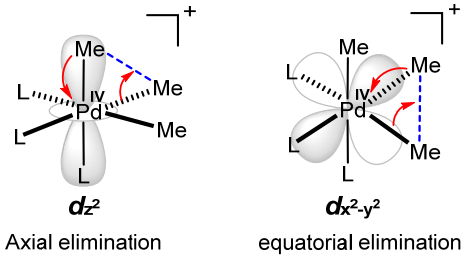

Scheme 8. Reductive elimination from intermediates **1**, **13**, and **7.** The C-C or C-O bond distances and activation energies are shown. [a]Due to the weak coordination of one Pd-pyridine (2.89Å) in the transition state. The two Me groups are differentiated as axial and equatorial. Therefore, this RE from **7** is a low-energy axial-equatorial RE consistent with our discussion above. Rotation to place the OH trans to pyridine to produce **7'** is not favorable.

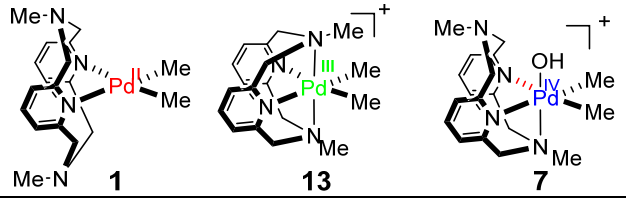

Bond Forming	Me-Me	Me-Me	Me-Me[a]	Me-OH
C-C (Å) /C-O(Å)	1.88	1.97	2.03	1.96
$\Delta G^{\neq}$(kcal/mol)	40.0	30.1	26.8	30.5

Additional calculations were carried out to evaluate RE from other potential candidates that have been detected in the reaction mechanism (eg. complexes **1**, **7** and **13**)[13]. As we anticipated, all these intermediates have higher activation energies and would not undergo RE at room temperature (Scheme 8). Thus complex **8** is only reasonable intermediate for RE to ethane. Reductive elimination is the fastest for high-valent Pd^{IV}, the rate increases with increasing oxidation state from Pd^{II} to Pd^{IV} (Scheme 8). The computations on RE of complex **7** indicate that the direct C-O bond formation is more difficult than C-C bond formation, a result that supports the recent report, by Vedernikov and co-worker, of yielding methanol in strong base.[12c]

CONCLUSION

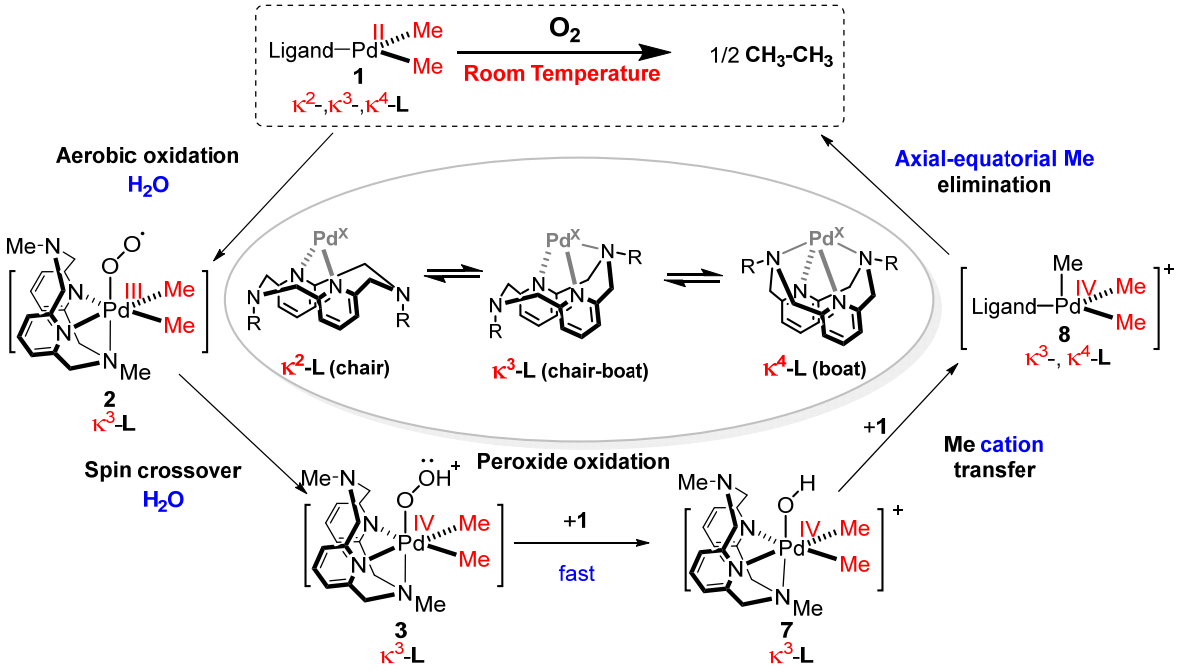

Figure 9. DFT confirmed mechanism of Aerobic Oxidative from Pd^{II} dimethyl complex to release ethane under mild condition.

In summary, this work describes the first detailed computational study on aerobic oxidation of tetradentate ligated Pd^{II} complex **1** to generate H_3C-CH_3 (Figure 9). The calculated mechanism suggests five key transformations in this reaction: (1) aerobic oxidation of Pd^{II} complex **1** to Pd^{III}–O_2^- complex **2**, (2) spin crossover between Pd^{III} complex **2** and Pd^{IV}–OOH complex **3**, (3) peroxidation of a Pd^{II} complex **1** by the Pd^{IV}–OOH complex **3**, (4) Me cation transfer from $Pd^{IV}Me_2OH$ complex **7** to Pd^{II} complex **1**, (5) reductive elimination of $Pd^{IV}Me_3$ complex **8**. From the computation on this mechanism, we discovered that H_2O (or other solvents, especially protonic ones) is essential to assist the aerobic oxidation by decreasing O_2 LUMO energy and stabilizing Pd-O_2 complex. Me cation transfer was suggested to be the more favorable than radical and anion pathways. For the final reductive elimination step, it is preferred that the axial-equatorial methyl releases ethane from Pd^{IV} complex **8**. Furthermore, ligand flexibility plays a significant

role and it is necessary to stabilize the most of intermediates and transition states, although in some case the contribution can be negative for a certain step (eg. reductive elimination prefers five coordination κ²-species). This flexibility leads to diverse axial coordination modes and provides a constructive clue to design new ligand systems, which would be critical to other chemical reaction such as late-stage C-H functionalization.[23] More studies toward conformational flexibility in chemistry are currently underway.

COMPUTATIONAL DETAILS

All quantum chemical calculations at the level of the density functional theory (DFT) were carried out with the Gaussiaon 09 Revision D.01 program package[24]. Molecular geometries were fully optimized by using the dispersion-corrected B3LYP-D3[25] functional without any symmetry constraints and broken symmetry approachs were employed for open-shell optimization. The effective core potentials (ECPs) of Hay and Wadt with a triple-ζ basis set (LANL2TZ) [26] were used for Pd, and the 6-31G(d, p) basis set was used for H, C, N and O (BS1). The energies were recalculated using a larger basis set (6-311++G (d, p) basis set for H, C, N and O) and triple-ζ basis set (LANL2TZ) for Pd (BS2) by single-point calculations, in implicit solvent treated with the universal solvation SMD model[27] and polarizable conductor CPCM model[28]. MeCN was used as solvent with a dielectric constant value of 35.688 and using UAHF (United Atom Hartree-Fock) radii for the respective atoms (Pd, H, C, N and O) in both SMD and CPCM calculations. For the part of O_2 coordination to Pd, calculated structures were fully optimized in SMD solvation model using B3LYP-D3/BS1 to better evaluate O_2 behavior in solvent. Basis set superposition error (BSSE) was also applied in this part. The minimum energy crossing points (MECP), here are spin cross point in Pd-O_2 complex, were calculated by structures scanning and the software developed by Harvey group [29].

All the structures were computed with the complete ligand structure as in the experiment. Additional density functionals such as B3LYP[30], M06L[31], M06[32] ω-B97XD[33], TPSS[34], TPSSh[34], were applied in selected intermediates and transition states to evaluate the functional influence. All optimized species were verified as either minima or

transition structures by the presence of zero or a single imaginary vibrational frequency. Free energies were evaluated at 298K using harmonic vibrational frequencies. Saddle points were connected to minima in the usual way with intrinsic reaction coordinate (IRC) calculations. The energies given throughout the paper are relative energy values computed with Gaussian 09 at 298 K and P=1 atm. Computed structures are displayed with CYLVIEW[35].

ASSOCIATED CONTENT

Supporting Information.

Optimized geometries of stationary points involved in energy profiles but not shown in the main text; comparison results for B3LYP, TPSS, TPSS*h*, M06 and M06L in optimized Pd-O_2 complex; test possible coordination Pd-O_2 complex; full calculated explicit solvent models of Pd-O_2 complex; scanned energy profiles of spin cross between triplet and singlet Pd-O_2 complex; spin density of Pd-O_2 complex with explicit solvent; comparison results for ωB97XD, B3LYP, B3LYP-D3 and M06L in reaction mechanism; mechanism of ligand flipping in more Pd^{IV} species; and the total energies and Cartesian coordinates of the structures involved in this study. This material is available free of charge via the Internet at http://pubs.acs.org

AUTHOR INFORMATION

Corresponding Authors

qpeng@nankai.edu.cn; mbhall@tamu.edu

Notes

The authors declare no competing financial interest.

ACKNOWLEDGMENT

The authors acknowledge financial support of The Welch Foundation (A-0648 to MBH) for initial support of this work. The majority of the work was supported by financial support from the Qatar National Research Fund under NPRP grant 7-297-1-051 to MBH and ENB. The work was completed with the help of National Natural Science Foundation

of China (21702109), "1000-Talent Youth Plan" of China, the European Community (FP7-PEOPLE-2012-IIF) under grant agreement 912364 to QP and the CSA-trust grant to QP. The authors acknowledge Texas A&M University's High Performance Research Computing Facility (http://hprc.tamu.edu/) for providing computing resources useful in conducting the research reported in this paper.

REFERENCES

(1) Clayden, J.; Greeves, N.; Warren, S.; Wothers, P. *Organic Chemistry* (1st ed.); Oxford University Press. USA. 2001, pp. 460–461.

(2) (a) Dubois, D. L. *Inorg. Chem.* **2014**, *53* , 3935–3960. And reference therein. (b) Theoretical predict catalyst: Fernandez, L. E.; Horvath, S.; Hammes-Schiffer, S. *J. Phys. Chem. Lett.* **2013**, *4*, 542–546.(c) Improved catalyst by Structural Dynamics:Cardenas, A. J. P.; Ginovska, B.; Kumar, N.; Hou, J.; Raugei, S.; Helm, M. L.; Appel, A. M.; Bullock, R. M.; O'Hagan, M. *Angew. Chem. Int. Ed.* **2016**, 55, 13509.

(3) (a) Crabtree, R. H. *Chem. Rev.* **1995**, *95*, 987. (b) Holmen, A. *Catal. Today* **2009**, *142*, 2. (c) Alvarez-Galvan, M. C.; Moto, N.; Ojeda, M.; Rojas, S.; Navarro, R. M.; Fierro, J. L. G. *Catal. Today* **2011**, *171*, 15.(d) Hammond, C.; Conrad, S.; Hermans, I. *ChemSusChem* **2012**, 5,1668.

(4) (a) Negishi, E. *Handbook of Organopalladium Chemistry for Organic Synthesis*; John Wiley & Sons: Hoboken, NJ, 2002; (b) van Leeuwen, P. W. N. M. *Homogeneous Catalysis: Understanding the Art*; Kluwer Academic Publishers: Dordrecht, 2004.

(5) (a) Miyaura, N.; Suzuki, A. *Chem. Rev.* **1995**, *95*, 2457. (b) Hartwig, J. F. *Organotransition Metal Chemistry: From Bonding to Catalysis*; University Science Books: Sausalito, 2010.

(6) (a) Stuart, D. R.; Fagnou, K. Science **2007**, *316*, 1172. (b) Yeung, C. S.; Dong, V. M. Chem. Rev. **2011**, *111*, 1215.

(7) (a)Liu, C.; Yuan, J.; Gao, M.; Tang, S.; Li, W.; Shi, R.; Lei, A. *Chem. Rev.* **2015**, *115*, 12138–12204.(b) Lehman, M. C.; Pahls, D. R.; Meredith, J. M.; Sommer, R. D.; Heinekey, D. M.; Cundari, T. R.; Ison, E. A. *J. Am. Chem. Soc.* **2015**, *137* , 3574–3584.(c) Xiao, D. J.; Gonzalez, M. I.; Darago, L. E.; Vogiatzis, K. D.; Haldoupis, E.; Gagliardi, L.; Long, J. R. *J. Am. Chem. Soc.* **2016**, *138*, 7161.

(8) (a) Stahl, S. S. *Angew. Chem., Int. Ed.* **2004**, *43*, 3400. (b) Stoltz, B. M. Chem. Lett. **2004**, *33*, 362. (c) Gligorich, K. M.; Sigman, M. S. *Chem. Commun.* **2009**, 3854. (d) Izawa, Y.; Stahl, S. S. *Adv. Synth. Catal.* **2010**, *352*, 3223. (e) Campbell, A. N.; Meyer, E. B.; Stahl, S. S. *Chem. Commun.* **2011**, *47*, 10257.(f) Campbell, A. N.; Stahl, S. S. *Acc. Chem. Res.* **2012**, *45*, 851–863.

(9) (a) Hull, K. L.; Lanni, E. L.; Sanford, M. S. *J. Am. Chem. Soc.* **2006**, *128*, 14047. (b) Canty, A., *J. Chem. Soc., Dalton Trans.* **2009**, 10409. (c) Chen, X.; Engle, K. M.; Wang, D.-H.; Yu, J.-Q. *Angew. Chem., Int. Ed.* **2009**, *48*, 5094. (d) Daugulis, O.; Do, H.-Q.; Shabashov, D. *Acc. Chem. Res.* **2009**, *42*, 1074. (e) Muniz, K. *Angew. Chem., Int. Ed.* **2009**, *48*, 9412. (f) Lyons, T. W.; Sanford, M. S. *Chem. Rev.* **2010**, *110*, 1147. (g) Sehnal, P.; Taylor, R. J. K.; Fairlamb, I. J. S. *Chem. Rev.* **2010**, *110*, 824.(h) Powers, D. C.; Ritter, T. *Top. Organomet. Chem.* **2011**, *35*, 129.(g) Topczewski, J. J.; Sanford, M. S. *Chem. Sci.* **2015**, *6* , 70–76.

(10) (a) McAuley, A.; Whitcombe, T. W. *Inorg. Chem.* **1988**, 27, 3090. (b) Chuang, G. J.; Wang, W.; Lee, E.; Ritter, T. *J. Am. Chem. Soc.* **2011**, *133*, 1760.

(11) Remy, M. S.; Cundari, T.; Sanford, M. S. *Organometallics* **2010**, *29*, 1522.

(12) (a) Boisvert, L.; Denney, M. C.; Hanson, S. K.; Goldberg, K. I. *J. Am. Chem. Soc.* **2009**, *131*, 15802–15814. (b) Petersen, A. R.; Taylor, R. A.; Vicente-Hernandez, I.; Mallender,′ P. R.; Olley, H.; White, A. J. P.; Britovsek, G. J. P. *J. Am. Chem. Soc.* **2014**, *136*, 14089–14099. (c) Sberegaeva, A. V.; Zavalij, P. Y.; Vedernikov, A. N. *J. Am. Chem. Soc.* **2016**, *138*, 1446–1455.

(13) (a) Khusnutdinova, J. R.; Rath, N. P.; Mirica, L. M, *J. Am. Chem. Soc.*, **2012**, *134*, 2414-2422.(b) Tang, F.; Zhang, Y.; Rath, N. P.; Mirica, L. M. *Organometallics*, **2012**, *31*, 6690-6696;(c) Tang, F.; Qu, F.; Khusnutdinova, J. R.; Rath, N. P.; Mirica, L. M. *Dalton Trans.*, **2012**, *41*, 14046-14050.

(14) (a) Zheng, B.; Tang, F.; Luo, J.; Schultz, J. W.; Rath, N. P.; Mirica, L. M. *J. Am. Chem. Soc.*, **2014**,*136*, 6499-6504;(b) Zhou, W.; Schultz, J. W.; Rath, N. P.; Mirica, L. M. M. *J. Am. Chem. Soc.*, **2015**, *137*, 7604-7607; (c) Zhou, W.; Rath, N. P.; Mirica, L. M. M., Dalton Trans., **2016**, *45*, 8693-8695; (d) Zhou, W.; Zheng, S.; Schultz, J.; Rath, N. P.; Mirica, L. M. M, . *J. Am. Chem. Soc.*, **2016**, *138*, 5777-5780.

(15) Khusnutdinova, J. R.; Rath, N. P.; Mirica, L. M. *Inorg. Chem.* **2014**, *53*, 13112–13129.

(16) Cheng, G. J.; Zhang, X.; Chung, L. W.; Xu, L.; Wu, Y. D. *J. Am. Chem. Soc.* **2015**, *137*, 1706–1725.

(17) (a)Popp, B. V.; Wendlandt, J. E.; Landis, C. R.; Stahl, S. S. *Angew. Chemie - Int. Ed.* **2007**, *46*, 601–604.(b) Popp, B. V.; Stahl, S. S. *Chem. - A Eur. J.* **2009**, *15*, 2915–2922.(c) Dang, Y.; Deng, X.; Guo, J.; Song, C.; Hu, W.; Wang, Z. X. *J. Am. Chem. Soc.* **2016**, *138* , 2712–2723.

(18) White, P. B.; Jaworski, J. N.; Fry, C. G.; Dolinar, B. S.; Guzei, I. A.; Stahl, S. S. *J. Am. Chem. Soc.* **2016**, *138*, 4869–4880.

(19) Lotz, M. D.; Remy, M. S.; Lao, D. B.; Ariafard, A.; Yates, B. F.; Canty, A. J.; Mayer, J. M.; Sanford, M. S. *J. Am. Chem. Soc.* **2014**, *136* 8237–8242.

(20) Mirica, L. M.; Khusnutdinova, J. R. *Coord. Chem. Rev.*, **2013**, *257*, 299-314.

(21) Boisvert, L.; Goldberg, K. I. *Acc. Chem. Res.* **2012**, *45* , 899–910.

(22) In our calculation, trying to eliminate two equatorial Me will automatically rotate to one axial and one equatorial Me.

(23) Topczewski, J. J.; Cabrera, P. J.; Saper, N. I.; Sanford, M. S. *Nature* **2016**, *531*, 220–224.

(24) Gaussian 09, Revision D.01, Frisch, M. J.; Trucks, G. W.; Schlegel, H. B.; Scuseria, G. E.; Robb, M. A.; Cheeseman, J. R.; Scalmani, G.; Barone, V.; Mennucci, B.; Petersson, G. A.; Nakatsuji, H.; Caricato, M.; Li, X.; Hratchian, H. P.; Izmaylov, A. F.; Bloino, J.; Zheng, G.; Sonnenberg, J. L.; Hada, M.; Ehara, M.; Toyota, K.; Fukuda, R.; Hasegawa, J.; Ishida, M.; Nakajima, T.; Honda, Y.; Kitao, O.; Nakai, H.; Vreven, T.; Montgomery, J. A., Jr.; Peralta, J. E.; Ogliaro, F.; Bearpark, M.; Heyd, J. J.; Brothers, E.; Kudin, K. N.; Staroverov, V. N.; Kobayashi, R.; Normand, J.; Raghavachari, K.; Rendell, A.; Burant, J. C.; Iyengar, S. S.; Tomasi, J.; Cossi, M.; Rega, N.; Millam, N. J.; Klene, M.; Knox, J. E.; Cross, J. B.; Bakken, V.; Adamo, C.; Jaramillo, J.; Gomperts, R.; Stratmann, R. E.; Yazyev, O.; Austin, A. J.; Cammi, R.; Pomelli, C.; Ochterski, J. W.; Martin, R. L.; Morokuma, K.; Zakrzewski, V. G.; Voth, G. A.; Salvador, P.; Dannenberg, J. J.; Dapprich, S.; Daniels, A. D.; Farkas, Ö.; Foresman, J. B.; Ortiz, J. V.; Cioslowski, J.; Fox, D. J. Gaussian, Inc., Wallingford CT, **2009**.

(25) Grimme, S.; Antony, J.; Ehrlich S. and Krieg, H. *J. Chem. Phys.*, **2010**, *132*, 154104.

(26) (a) Hay, P.J. and Wadt, W.R. *J. Chem. Phys.* **1985**, *82*, 299. (b) Roy, L.E.; Hay,P.J. and Martin, R.L. *J. Chem. Theory Comput.* **2008**, *4*, 1029.

(27) Marenich, A. V.; Cramer,C. J.; and Truhlar, D. G. *J. Phys. Chem. B*, **2009**, *113*, 6378-96 .

(28) Cossi, M.; Rega, N.; Scalmani, G.; and Barone, V. *J. Comp. Chem.*, **2003,** *24,* 669-81.

(29) Harvey, J.N.; Aschi, M.; Schwarz, H.; Koch, W. *Theor. Chem. Acts.*, **1998**, *99*, 95.

(30) (a) Becke, A. D. *Phys. Rev.* **1988**, *A38*, 3098. (b) Becke, A. D. *J. Chem. Phys.* **1993**, *98*, 1372. (c) Becke, A. D. J. Chem. Phys. **1993**, *98*, 5648. (d) Lee, C.; Yang, W.; Parr, R. G. Phys. Rev. **1988**, *B37*, 785.

(31) Zhao, Y.; Truhlar, D. G. *J. Chem. Phys.* **2006**, *125*, 194101: 1.

(32) Zhao, Y.; Truhlar, D. G. *Theor. Chem. Acc.* **2008**, 120, 215.

(33) Chai, J.-D.; and Head-Gordon, M.; *Phys. Chem. Chem. Phys.* **2008,** *10*, 6615.

(34) Tao, J. M; Perdew,J. P.; Staroverov, V. N.; and Scuseria,G. E.; *Phys. Rev. Lett.*, **2003,** *91*, 146401.

(35) CYLview, 1.0b; C. Y. Legault, Université de Sherbrooke, 2009 (http://www.cylview.org).

TOC

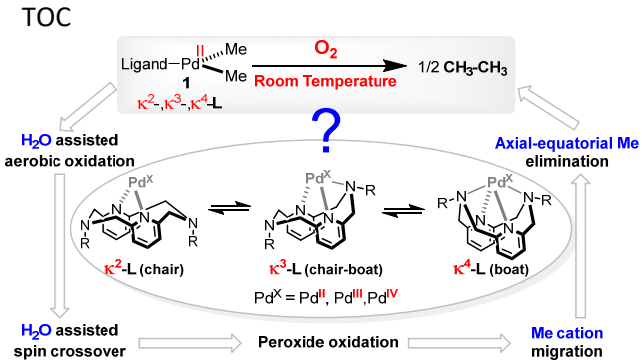
Ligand—Pd(II)(Me)(Me)
1
κ2-,κ3-,κ4-L
O2
Room Temperature
1/2 CH3-CH3
?
H2O assisted aerobic oxidation
Axial-equatorial Me elimination
κ2-L (chair)
κ3-L (chair-boat)
κ4-L (boat)
PdX = PdII, PdIII,PdIV
H2O assisted spin crossover
Peroxide oxidation
Me cation migration